Journal of Applied Polymer Science

WILEY

Applied Polymer SCIENCE

RESEARCH ARTICLE OPEN ACCESS

Assessing the Integrity of N95 Mask Elastomer Straps With Decontamination and Reuse

Ian Pelse[1] | Zach D. Seibers[2] | John R. Reynolds[1,2] | Meisha L. Shofner[1]

[1]School of Materials Science and Engineering, Georgia Institute of Technology, Atlanta, Georgia, USA | [2]School of Chemistry and Biochemistry, Georgia Institute of Technology, Atlanta, Georgia, USA

Correspondence: Meisha L. Shofner (meisha.shofner@mse.gatech.edu)

Received: 13 September 2024 | **Revised:** 28 November 2024 | **Accepted:** 9 December 2024

Funding: This work was supported by the National Science Foundation, CMMI-2031545, ECCS-2025462.

Keywords: decontamination | elastomers | ozone

ABSTRACT

The rapid progression of the COVID-19 pandemic revealed an inability to meet increased demand for N95 respirators. These respirators are designed to be used once and disposed, but throughout the pandemic, there was a need for their decontamination and reuse. This research investigates the effect of various decontamination methods on the chemical and mechanical properties of N95 mask straps made of natural rubber to explore how these straps change after decontamination and what materials characterization techniques are well-suited to evaluate these changes. Using results from ozone decontamination, tensile testing of mask strap assemblies is identified as the most reliable way to quantify changes in strap properties with decontamination and reuse when compared to other analytical techniques. Additionally, visible strap degradation often precedes both strap failure and material property changes and can be a reasonable indicator to discontinue use. Aside from ozone, decontamination with other methods such as heat and UV light appears to be less damaging to the tested materials. Beyond the specific results presented, this study provides insight on testing strategies that can be employed to move forward with evaluating new materials and decontamination methods for use in future pandemics or in more resource-limited regions.

1 | Introduction

During the height of the COVID-19 pandemic, crucial personal protective equipment (PPE) such as N95 masks was in short supply in industries including healthcare, emergency response, and other essential sectors. As a result, there was a need to reuse these masks, which are generally designed to be used only once and then discarded [1]. In the time since the initial surge of COVID-19, PPE shortages in the United States have been in large part resolved; however, the experience gained during COVID-19 suggests that PPE reuse may be needed in a future pandemic. Research on N95 mask efficacy has shown them to be superior in preventing viral transmission in settings outside healthcare environments compared to surgical or cloth masks, suggesting a broader impact for implementing decontamination protocols of N95 masks [2]. While the development of practical, low-cost strategies for the reuse of PPE has wide-ranging societal benefits, it would be especially beneficial in parts of the world with limited resources and large population densities. Knowledge of reuse strategies will not only provide lifesaving information now, but also enable the redesign of future protective masks to reduce the use of single-use plastics and increase the availability of PPE for global healthcare needs.

Safe reuse of PPE requires the cleaning of surfaces that could be contaminated with the coronavirus SARS-CoV-2. Some techniques explored for N95 respirator decontamination include the following: vaporized hydrogen peroxide (VHP) [3, 4], ultraviolet radiation (UV) also known as ultraviolet germicidal irradiation (UVGI) [5, 6], heat (which can be either

humid or dry) [7], steam [8], ozone [9–11], and chlorine dioxide [12, 13]. Several groups have studied the efficacy of the filtration medium over the course of repeated decontamination cycles among these various techniques, but less effort has focused on understanding how these treatments affect the integrity of the mask straps specifically [11, 14–16]. Retaining the mechanical and chemical integrity of the mask strap is vital in ensuring a tight seal between the face and the mask, and therefore critical to achieving the expected air filtration performance of a N95 respirator.

Reuse of respirators and other forms of PPE in hospitals was authorized during the COVID-19 pandemic by the Food and Drug Administration under Emergency Use Authorizations (EUA) following decontamination with methods such as VHP, UVGI, and moist heat [17]. Along with those techniques, ozone has also been shown to deactivate SARS-CoV-2 [18], and the integrity of N95 filtration media has been determined to be maintained over at least 10 ozone decontamination cycles [9]. The main material comprising the N95 mask filtration media is a polypropylene/polyester blend [19], which has been shown to be chemically robust to ozone treatment [20]. On the other hand, polyisoprene rubber, often used as a mask strap, is known to degrade in the presence of ozone [21]. Increasing the ambient humidity during the ozone treatment, which increases the efficiency of the decontamination process, also contributes to this degradation [22]. In work by Blanchard et al., by way of studying N95 mask performance as a function of ozone decontamination treatment, certain mask straps were found to degrade at the stapled attachment before even one decontamination cycle was completed [9]. This localized degradation was likely due to the additional strain on the strap at this point. The same group found that putting the complete band under a large amount of tension (240% strain) during exposure resulted in significant degradation and loss of mechanical integrity. This result is consistent with early reports of natural rubber reactions with ozone. In those studies, relaxed rubbers showed minimal changes in morphology and mechanical properties with ozone exposure as compared to rubbers exposed under strain, where cracks were likely to develop rapidly and compromise bulk material properties [22, 23].

Mechanical integrity concerns are not limited to ozone use, and other decontamination methods such as heat and UVGI can also degrade rubber mask straps. We considered these techniques for our work due to the relative ease with which they could be implemented in a laboratory setting. Treating contaminated surfaces with either of those methods has been well documented, especially in the context of reusing PPE in pandemics. These techniques have been tested via the decontamination of enveloped viruses such as H1N1 [24] and H5N1 [25] in controlled settings to ensure a consistent treatment dose. Like ozone treatment, heat treatment can be effective in dry or moist conditions, but moist heat appears to be more effective in deactivating viruses in otherwise identical treatment conditions [26, 27]. Performance of the N95 filtration media is maintained with up to 20 cycles of dry heat treatment [28], but the mask strap integrity has not been similarly characterized. Work on characterizing the effect of UVGI treatment on N95 respirators is similar. The effectiveness of the filtration media is well characterized on its own but not with respect to the integrity of the mask straps [6].

Considering each decontamination technique, establishing protocols for practical decontamination and therefore the conditions that the mask will experience during decontamination is crucial in designing laboratory experiments that properly simulate usage. While having the mask strap strained during exposure is not necessarily required for decontamination, there are certain instances when the strap may be under load during a specific decontamination technique. While the strain is not likely to be 240% as used in the previously mentioned ozone study [9], a smaller amount of strain may still lead to degradation of the strap. Given the crucial importance for mask operation and the sensitivity of elastomeric materials to ozone (and many other decontamination techniques), there remains a critical void in understanding how to practically assess strap damage in the field and develop guidelines for mask users.

In this work, we seek to address this knowledge gap by investigating materials characterization techniques for their ability to establish relationships between decontamination treatments, fundamental polymer properties, and practical elastomer behavior. This work seeks to reveal indicators of strap failure and identify changes in strap properties with decontamination that could precede catastrophic failure and the need for mask disposal. This information will be useful in the development of tests to inform guidelines for reusing masks as many times as possible. Through characterization of the chemical structure and physical properties of the materials before and after decontamination, we elucidated dependencies on the elastic strap degradation under different decontamination conditions. For decontamination with ozone, we observe some chemical and material property changes with increasing decontamination. Additionally, we address alternative decontamination methods, specifically heat and UV-C treatments, and show that mask straps can be more robust to these methods compared to ozone treatment. Overall, these results showed that mechanical testing methods were sensitive to changes in strap and mask strap assembly properties, whereas other methods provided less definitive guidance about material changes resulting from decontamination methods.

2 | Experimental Section

Due to supply restrictions over the course of this work, the testing was performed on a single type of N95 mask. The specific N95 mask used was Moldex 2200 N95 (McMaster-Carr). According to the product documentation, the strap is made from natural rubber latex, which would indicate that the straps were polyisoprene. Ozone decontamination was performed with a ZONO SC 1 ozone cabinet from Zono Technologies. Over the course of a 20-min decontamination cycle, the cabinet maintains an average ozone concentration of 22 ppm at a relative humidity of 75%. This procedure has been shown to deactivate the enveloped respiratory virus influenza A, which is a suitable surrogate for SARS-CoV-2 [9]. Ozone treatment has also been shown to disinfect surfaces contaminated with SARS-CoV-2 [18].

As alternatives to ozone, decontamination with dry heat and UV was also examined. Heat decontamination was performed with a laboratory oven set to 100°C, with one cycle lasting for 50 min, which has been shown to deactivate enveloped viruses [28].

UV decontamination was performed with UV-C light using an American Ultraviolet Co. lamp model CE-25-4H, with Phillips TUV 25W/G25T8 mercury bulbs. Light intensity at 254 nm was measured with a Newport Power Meter Model 843-R and a Newport 818-RAD Irradiance and Dosage Sensor, to confirm irradiance of ~15 mW/cm^2 along all the straps including the stapled attachment. To decontaminate the material, a UV-C irradiation dose of 1.0 J/cm^2 is required, which is achieved after 66 s at the specified irradiance [29]. However, there have been reports of residual virus being found on the straps after decontamination, which is likely due to portions of the respirator or strap being blocked from the light source [6, 30]. Therefore, it is recommended to wipe down the strap with a suitable disinfectant; to meet this recommendation, we performed the UV-C decontamination with and without wiping the straps with 80% ethanol after each cycle.

Cyclic tensile testing was performed on an Instron 5566 Universal Testing Machine, using a 100-N static load cell. For testing where the strap was attached to the mask, a rubber roller grip was used on the top of the test frame to grip the strap, and a mechanical wedge action tensile grip was used to grip the mask. The attachment of the strap to the mask was not altered from its manufactured condition. The gauge length varied somewhat between samples, and these differences are noted in the discussion of the results. When gauge lengths were the same, quantitative comparisons were made between samples, whereas only qualitative comparisons were made if gauge lengths were different. Prior to treatment and measurement, the mask strap assemblies were prestretched to 100% strain for approximately 5 min.

Tensile set experiments similar to the ASTM D412 standard for characterizing vulcanized thermoset rubbers were performed on the mask assemblies. The mask strap was stretched at a rate of 5 mm/s to 100% strain where it was held for 3 min. This hold time was sufficient for the stress relaxation phenomena to subside and the stress to stabilize. After 3 min, the strap was relaxed to the point at which the stress was 0 MPa, which occurred at a positive strain due to tensile set of the elastomer. After a 3-min rest, the loading and unloading cycle with holds was repeated several times until the sample failed or the desired number of cycles was reached, in most cases five or six cycles. Figure S1 shows 21 cycles of the tensile set test for an N95 mask strap to illustrate the testing method.

Images of the mask straps were obtained with an optical microscope (Olympus BX51). Samples were imaged in their relaxed state and while stretched. An untreated sample and a sample exposed to one ozone decontamination cycle were imaged for comparison.

The chemical structure of the mask straps was examined with Fourier transform infrared spectroscopy (FTIR) using a Shimadzu Prestige 21 FTIR instrument with an attenuated total reflectance (ATR) attachment. Spectra were obtained over a wavenumber range of 3500 to 700 cm^{-1} using a resolution of 2 cm^{-1} and a Happ-Genzel apodization function. Thirty-two scans were averaged per measurement. Samples were characterized with ATR-FTIR in their untreated condition and after seven cycles of ozone treatment.

Dynamic mechanical analysis (DMA) temperature scan experiments were performed using a Mettler Toledo DMA/SDTA861e in tension mode with a small clamping assembly sample holder. The samples were die cut using the gauge section of an ASTM D638-V die to ensure that the geometries of all samples were the same in the test region, which was 9.0 mm in length and ~3.2 mm in width. The die-cut samples were trimmed at the ends to ensure fit in the clamping assembly but were not trimmed in the measurement region to preserve the integrity of the die cut. DMA scans were conducted over a temperature range of −75°C to 25°C at 2°C/min using a frequency of 1 Hz. In some cases, the lower-temperature data were truncated to eliminate values that were obtained before the temperature stabilized. The tests were conducted in the linear viscoelastic regime using limits of 0.1 N or 10 μm. The instrument switched between these limits as the temperature increased to accommodate changes in the stiffness of the material.

Solvent swelling experiments were performed with ACS grade toluene, with samples on the order of 20–50 mg topped with toluene, sealed in vials, and left in the dark for 5 days. The samples were then allowed to drip dry before being weighed. The change in mass was represented as the mass increase divided by the original mass before solvent exposure. Five samples were tested.

3 | Results and Discussion

As we explored changes that occurred over multiple decontamination cycles, we established a few different conditions for comparison. We considered up to 10 decontamination cycles with ozone, heat, and UV-C as a reasonable window for mask reuse, given existing evidence that the filtration media should function up to that point with several different decontamination methods [8]. Aside from number of doses, we also considered the strain of the strap during decontamination. The previously mentioned study on mask integrity stretched the band to over twice its original length during decontamination, just as a proof of concept to demonstrate the issue [9]. Based on our experience with the masks, a strain of 200% represented the approximate strain required to fit a mask over one's head and was an extreme condition that caused complete strap failure in very few decontamination cycles. However, based on reported implementations, we did not envision the need to stretch a face mask strap to that great of an extent during decontamination. We have instead investigated a more realistic strain during decontamination of 10% strain for samples subjected to one ozone treatment cycle and samples subjected to three ozone treatment cycles. This small strain could simulate the phenomena of suspending the mask on a rack via its straps, as seen with the previously mentioned UV decontamination [29]. Straps were also tested after exposure to two ozone decontamination cycles, and these straps were not strained during decontamination.

We used tensile testing of the mask strap attachment to uncover the behavior of the complete mask assembly and its performance with successive decontamination cycles. The resulting stress–strain curves from this experiment as a

function of number of ozone cycles are shown below in Figure 1. Considering the untreated mask strap, the stress at 100% strain after the first stretch is ~1.6 MPa, while after the second strain cycle, the stress dropped to ~1.5 MPa. This stiffness loss upon load cycling, which simulates mask use and reuse, leads to stress softening and hysteresis, a phenomenon known as the Mullins effect [31, 32]. As observed for other elastomers, the stress drop between the first and second cycle was substantial, and changes with subsequent cycles were less significant. Qualitatively, similar hysteresis was seen for the untreated strap (Figure 1a) as well as the strap that had undergone one ozone treatment (Figure 1b). The gauge lengths of these two samples were different (150 mm for the untreated strap and 130 mm for the strap exposed to one ozone cycle), so a quantitative comparison of the stress values was not made. However, the overall behavior was similar in that both samples did not fail over the course of the experiment (in this case six loading and unloading cycles) and curve shapes were similar.

The behavior of the strap after two ozone treatments was markedly different and showed earlier failure. After these two ozone cycles, strap degradation tended to occur at the attachment point; however, it was often accompanied by non-uniform damage throughout the entire strap. Two examples of this are shown: The inset in Figure 1c shows a photograph of this strap during the experiment but before failure, while another example with a larger view is shown in Figure S2. The two ozone dose data in Figure 1c show a strap that has failed during the fourth holding step, but we have also observed failure during the third holding step in a separate test. Additionally, the gauge length of the sample shown in Figure 1c was the same as that for the strap exposed to one ozone treatment (Figure 1b); therefore, their stress values could be compared. After two ozone treatments, the maximum stress achieved was lower (~1.6 MPa for one ozone exposure and ~1.3 MPa for two ozone exposures), further indicating degradation of the material. Finally, the mask straps that had undergone three ozone cycles completely failed the stretch test; three different strap samples failed during the initial stretch, with the earliest occurring at only ~10% strain (Figure 1d). These results suggested that for this mask strap, two ozone treatments compromised reuse and any further decontamination cycling with ozone led to catastrophic failure. We also verified our testing methodology of dosing multiple times before any mechanical testing, which was different than a proper use case of mechanical stress after each decontamination, and conducted a separate test with stretching included between decontamination cycles. For this experiment, the mask strap assembly was stretched to 100% extension and held for 10 min after each decontamination cycle. The results of this experiment are presented in Figure S3. The mask strap assembly performed similarly to the strap exposed to two ozone cycles without stretching between exposures shown in Figure 1c, failing during the fourth holding step though the loading curve showed increased stress values at

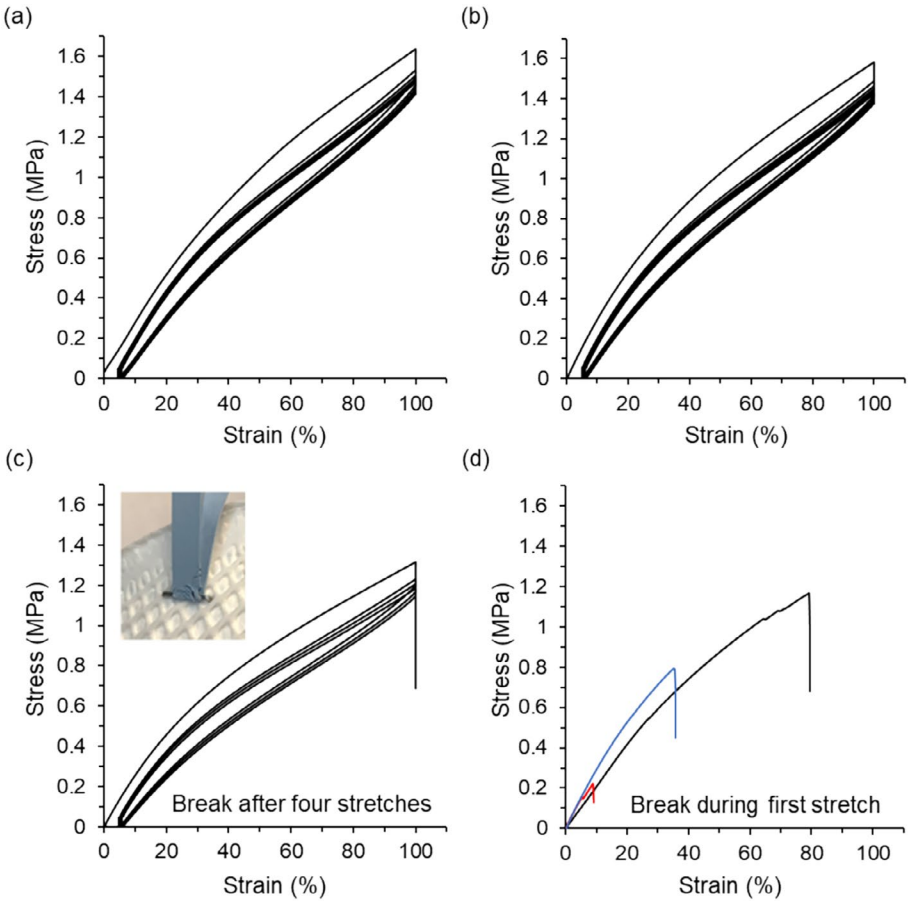

FIGURE 1 | N95 mask strap tensile testing as a function of decontamination cycle. One test is shown for the untreated (a), one ozone dose (b), and two ozone doses samples (c), while three separate tests are shown for the three ozone doses samples (d), which break upon the first stretch. An example of the degraded two ozone-dosed straps during cycling but before failure is shown as an inset of (c). [Color figure can be viewed at wileyonlinelibrary.com]

extensions larger than ~50 mm. This methodology was not equivalent to the use case where one may wear the mask for a longer period of time, but it suggested that our methodology was suitable to monitor the progression of strap failure with decontamination.

As stated earlier, the samples examined with this testing were mask strap assemblies as opposed to strips of the mask strap material, so the cyclic tensile testing investigated the response of the system as opposed to just the mask strap material. With this distinction in mind, we also constructed the plots of the stress during the first tension cycle as a function of extension instead of strain to compare the assemblies and complement the cyclic stress–strain data. These data for the untreated strap and the strap exposed to one or two ozone cycles are shown in Figure S4 and include multiple samples for each condition. In this visualization, the highest extension value shown corresponded to the gauge length of the sample; thus, the samples had different extension value ranges since their gauge lengths differed. Comparing the stress–extension curves, the three untreated strap samples showed similar behavior in that their stress–extension curves had similar shapes and followed similar trends. The straps subjected to one ozone cycle showed more variability in the response with two of the samples more similar to the untreated strap and two other samples with lower stress values over the extension range. The straps subjected to two ozone cycles were similar to each other, and after initial deformation, these straps had lower stress values than the untreated straps.

To observe the damage incurred by ozone exposure, we observed the untreated and treated straps with optical microscopy. Optical micrographs of the mask straps are shown in Figure 2. The treated sample was exposed to one ozone cycle while being held at 10% strain. The straps were imaged in a relaxed state as well as in states of increasing strain in order to examine the various textures in the sample. The untreated strap appeared the same in the relaxed state and at the two strain levels used in this work. The surface was smooth, and no cracks were observed. However, the treated strap showed a different behavior. In the relaxed state, visible cracks were observed in the treated strap. As the treated strap was stretched under the microscope, a heterogeneous network was observed with the surface separating to reveal an internal structure holding the strap together, indicating that the ozone-induced degradation was experienced preferentially at the surface and providing further insight into the failure observed with tensile testing.

DMA, a thermomechanical testing technique, was also used to observe changes in material structure caused by ozone exposure by characterizing the viscoelastic response of the materials and providing a measurement of the glass transition temperature (T_g). The viscoelastic response of the material is primarily captured in DMA through calculation of three quantities: the storage modulus (E'), the loss modulus (E''), and tan delta. E' and E'' provide information about the elastic and viscous contributions to the viscoelastic response, respectively. Tan delta is the ratio of E'' to E' and can be a measure of damping. Additionally, E'' and tan delta data were used to quantify T_g, which is a fundamental property of the polymer and helps explain the physical behavior of a macro-scale polymer sample, here being a mask strap. For a material that is rubbery at ambient conditions, T_g occurs at lower

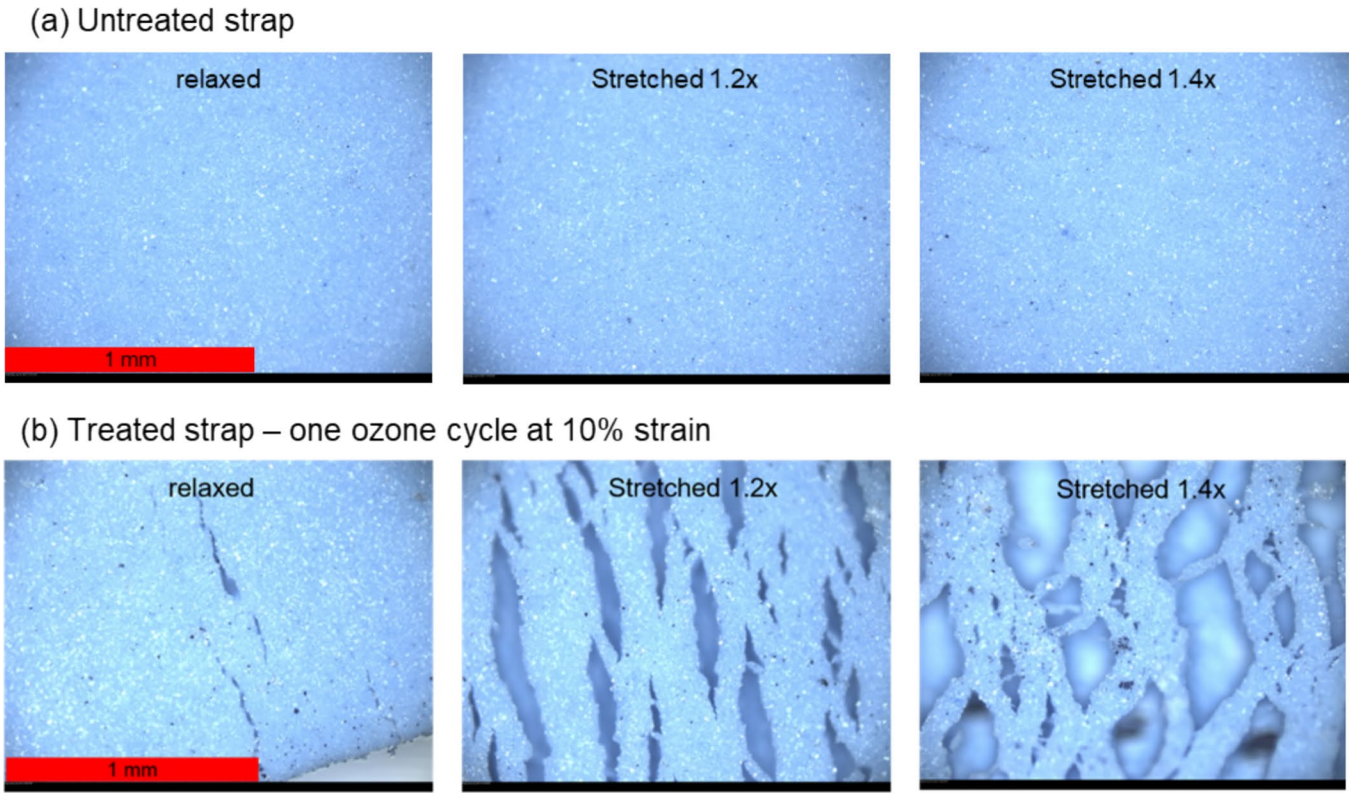

FIGURE 2 | Optical micrographs of the N95 mask strap in the untreated condition (a) and after one ozone cycle at 10% strain (b). Band stretched progressively from left to right, highlighting the inhomogeneous degradation and the voids that emerge in the strap subjected to ozone treatment. [Color figure can be viewed at wileyonlinelibrary.com]

temperatures than an N95 face mask will experience during normal operation. However, we can compare changes in the glass transition to assess changes in the material's structure and mechanical integrity. DMA is a useful technique for measuring T_g because it directly tracks the fundamental molecular processes of the glass transition, that is, the onset of segmental motion.

The temperature scan DMA data for the untreated and ozone-treated straps are shown in Figure 3. The samples shown are an untreated mask strap, a strap exposed to one ozone cycle at 10% strain, and a strap exposed to three ozone cycles. Examining the values of storage modulus, the curve shapes of the three samples were largely similar, and the strap exposed to three ozone cycles showed the most significant difference when compared to the untreated strap. The strap exposed to three ozone cycles failed immediately upon use during the cyclic tensile test experiments, so these results support that a change in properties resulted from exposure to repeated ozone decontamination. However, an increased E' value suggests that the degradation associated with ozone exposure led to stiffening. An increased stiffness would be contrary to the expected degradation pathway of chain scission through reactions between ozone and carbon double bonds. However, some work has suggested that natural rubber degradation due to ozone exposure proceeds by both pathways sequentially, with increases in crosslinking occurring at initial dosing and then chain scission occurring with further exposure [33].

T_g values based on the peak from the E'' data were consistent with the results from E' data. As shown in Figure 3b, the values of T_g were − 53.2°C, −52.3°C, and −51.5°C for the untreated strap, the strap subjected to one ozone treatment, and the strap subjected to three ozone treatments, respectively. The T_g values for the untreated strap and the strap exposed to one ozone cycle were similar to each other, but three ozone exposures produced a small increase in T_g, suggesting that crosslink density could have increased with ozone exposure. Additionally, the peak shapes were largely similar for the three samples, indicating that the breadth of the glass transition did not change substantially and any changes in crosslink density caused by ozone exposure led to restrictions in polymer mobility that affected the material uniformly in this test.

Similar behavior was observed in the tan delta data, though differences in the values were smaller, suggesting that any changes in polymer structure were slight. Values of T_g from the peak of tan delta were − 45.6°C, −45.4°C, and − 44.8°C for the untreated strap, the strap subjected to one ozone treatment, and the strap subjected to three ozone treatments, respectively. Overall, the DMA data (E', E'', and tan delta) indicated that some changes in polymer structure could have occurred with repeated ozone exposure, but the results were not as conclusive as those obtained with cyclic tensile testing.

We used ATR-FTIR to characterize the chemical structure of materials that were exposed to ozone. The spectra for the mask straps are shown in Figure 4, both in the untreated case and after seven ozone cycles, a harsher condition than previously used. The spectra had features consistent with the structure of polyisoprene: bands in the 2800–3000 cm^{-1} region corresponding to C-H stretch, a band near 1660 cm^{-1} corresponding to C=C stretch, and a band at 838 cm^{-1} corresponding to C-H wag [34]. Comparing the spectra for the untreated strap and ozone-treated strap, three absorption bands showed distinguishable changes (1539, 1456, and 1375 cm^{-1}). These bands were associated with the carboxylate anion in zinc stearate [35]. Zinc stearate is an additive used as an activator for sulfur-based curing, and it would be expected to find this compound in the strap material. The intensity of these bands increased following ozone exposure, with the intensity of 1539 cm^{-1} showing the largest difference. Previously published work concerning ozone decontamination of polyisoprene also showed an increased intensity of the band at 1539 cm^{-1} for polyisoprene exposed to ozone at high humidity and attributed this increase to migration of zinc stearate to the exposed surface [36]. Considering other features of the spectra, no change in crosslink density was evident from these data since the intensity and shape of the absorption band near 1660 cm^{-1} were not changed with ozone exposure. Since limited changes in the polyisoprene structure were detected beyond an increased presence of zinc stearate, we concluded that using FTIR as a method to describe explicit relationships between ozone exposure and chemical structure would be challenging.

To look at the bulk strap changes in a different way, we used solvent swelling to measure the interactions between the untreated and ozone-treated elastomers and a compatible solvent. In this experiment, the polymer should uptake more solvent and swell more if the network structure experienced chain scission during decontamination [37–39]. The opposite result would occur if

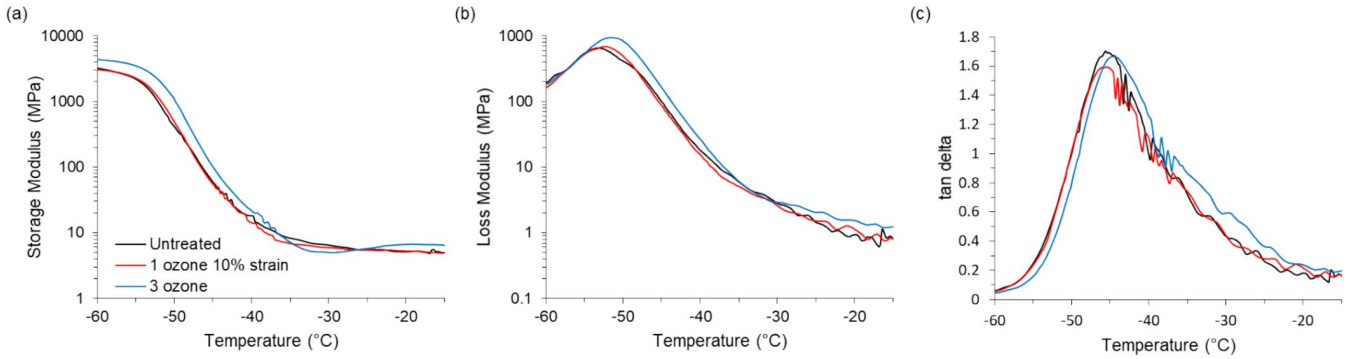

FIGURE 3 | Storage modulus (a), loss modulus (b), and tan delta (c) data from DMA temperature sweep experiments, comparing the untreated strap, a strap at 10% strain exposed to one ozone cycle, and a strap exposed to three ozone cycles. [Color figure can be viewed at wileyonlinelibrary.com]

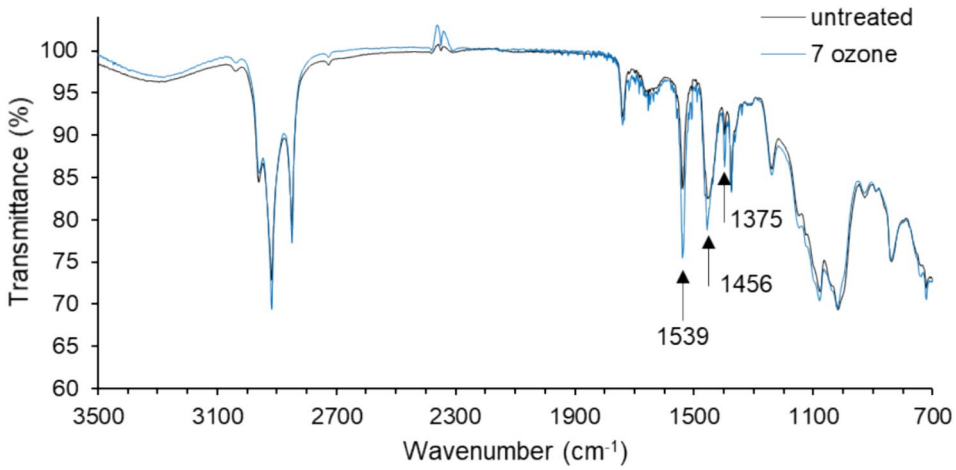

FIGURE 4 | FTIR spectra of N95 mask strap in the untreated condition (black) and after seven ozone cycles (blue). [Color figure can be viewed at wileyonlinelibrary.com]

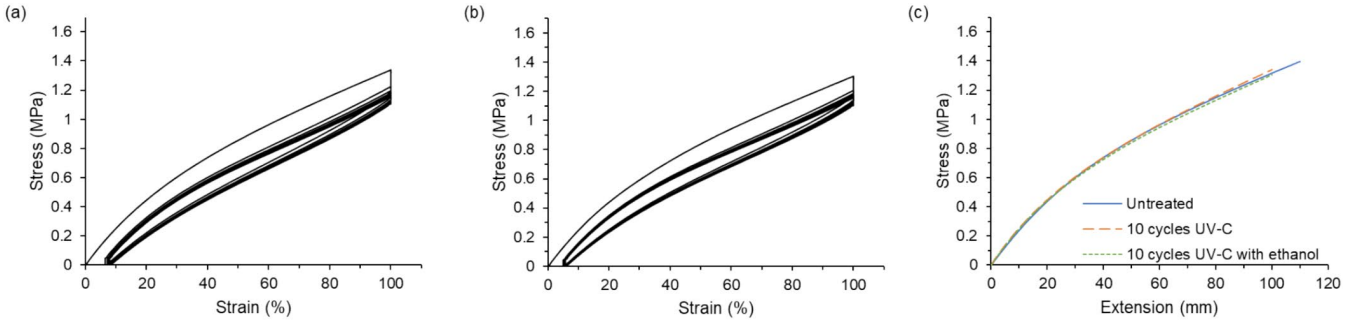

FIGURE 5 | Tensile testing of the mask strap assembly after (a) 10 UV-C cycles and after (b) 10 UV-C cycles with ethanol cleaning after each decontamination cycle. Stress–extension curves are shown in (c) to compare to an untreated mask strap with a similar gauge length. [Color figure can be viewed at wileyonlinelibrary.com]

crosslink density increased. Examining the mass increase of the samples shown in Figure S5, we observe no meaningful trend between extent of decontamination and mass increase for the mask strap material with large, overlapping error bars.

We have shown above that results from DMA, ATR-FTIR, and swelling experiments did not show clear changes in elastomer properties with decontamination and thus were not necessarily able to predict eminent strap failure in a practical setting. Additionally, these methods might not capture the effects of inconsistent degradation at various locations (including at the attachment point) on the elastic straps that was observed from visual inspection. These results supported the continued use of cyclic tensile testing as the primary characterization method for assessing different decontamination methods. With this in mind, we explored two other decontamination techniques as a comparison: dry heat treatment and UV-C treatment. Following decontamination, we performed the cyclic tensile testing as previously described.

Stress–strain curves and a combined stress–extension curve for the mask strap assemblies that have undergone 10 cycles of either UV-C treatment or UV-C with ethanol cleaning are shown in Figure 5. An untreated strap with a more similar gauge length is included for comparison in the stress–extension plot shown in Figure 5c as well. Treatment with 10 UV-C cycles resulted in little change from the untreated strap. Additionally, including a step to wipe the strap with ethanol after each decontamination cycle did not change the strap's response to stress cycling. Since there was a small difference in gauge length for the samples compared (110 mm for the untreated straps and 100 mm for the straps treated with UV-C or UV-C with ethanol), the maximum stress values for the treated straps were not compared quantitatively to the untreated strap; however, the behavior was similar in that the straps were able to withstand six stretching cycles. The stress–extension curves shown in Figure 5c indicated that the untreated mask strap assembly and the mask strap assemblies treated with either UV-C decontamination protocol had similar stiffness in the first stretching cycle, further suggesting that 10 cycles of UV-C treatment had minimal impact on the behavior. To investigate whether further treatment might cause changes in mechanical behavior, treatment with 20 UV-C cycles was also pursued, and the results of the stress cycling test are shown in Figure S6. This strap had the same gauge length as the strap subjected to 10 UV-C cycles, so the maximum stress values for the straps treated with UV-C could be compared. Overall, the strap was able to withstand the stress–cycling test after 20 UV-C cycles, but the maximum stress attained was lower. The strap that experienced 20 cycles had a maximum stress value of ~1.2 MPa, and the strap that experienced 10 cycles had a maximum stress value of ~1.3 MPa, suggesting some weakening of the strap with prolonged exposure to UV-C.

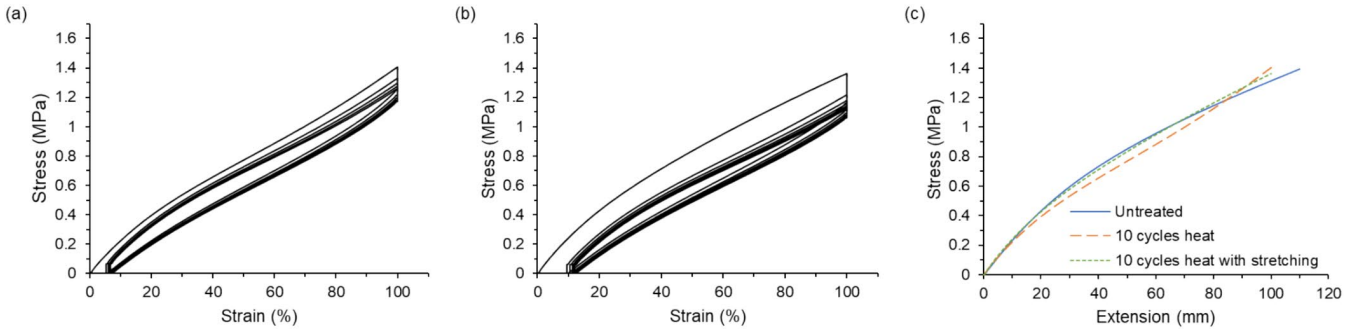

FIGURE 6 | Tensile testing of the mask strap assembly after (a) 10 heat cycles and after (b) 10 heat cycles with stretching after each decontamination cycle. Stress–extension curves are shown in (c) to compare to an untreated mask strap with a similar gauge length. [Color figure can be viewed at wileyonlinelibrary.com]

Heat treatment showed a similar result to UV-C treatment in that 10 cycles heat exposure did not lead to premature failure of the mask strap assembly. Figure 6 shows the stress–strain curves for a sample exposed to 10 heat decontamination cycles (Figure 6a) as well as a sample exposed to 10 heat decontamination cycles with a stretching step added between cycles (Figure 6b). These samples had the same gauge length, so their maximum stress values could be compared. The sample with stretching steps included between decontamination cycles had a slightly lower maximum stress than the strap that did not experience stretching between decontamination cycles; however, both values were ~1.4 MPa. These values are comparable to the straps exposed to 10 UV-C cycles. Another sample was prepared and subjected to 20 heat decontamination cycles to observe the effects of prolonged exposure. Its stress–strain curve is shown in Figure S6. While this sample did not fail during the test, we observed a lower maximum stress for this strap, ~1.2 MPa. Overall, the alternate decontamination protocols used in this work were less damaging than ozone treatment, and the mechanical testing protocol was able to ascertain differences in the performance of the mask strap assembly.

4 | Conclusion

In this work, we characterized the chemical and mechanical changes in a mask strap elastomer material after ozone decontamination with a goal of understanding which characterization experiments would be best suited to assess changes in material behavior from ozone exposure. Of the techniques investigated in this work, cyclic tensile testing was found to reliably detect performance changes in mask strap assemblies following ozone exposure. Additionally, the results of this testing demonstrated that typical mask strap elastomers were likely to fail at the stapled attachment, but bulk failure was also commonly observed due to visible inhomogeneities in the strap that could nucleate and concentrate degradation processes. Results from DMA, FTIR, and swelling experiments showed smaller changes in their respective indicators, suggesting that these techniques would be of less utility in this application. Using the cyclic tensile testing protocol, we also reported that the mask straps tested here were significantly more robust to heat and UV-C treatment when compared to ozone.

Beyond the specific results presented in this paper, future work should investigate the behavior of other mask strap materials and attachment mechanisms since these variables in mask design may cause a mask assembly to respond differently to decontamination protocols. Additionally, future work examining the effects of different storage conditions and environmental conditions during use on mask performance and subsequent reuse after decontamination may provide different results that could assist with PPE reuse globally. Considering the many mask designs and materials of construction available, the results of this study provide an initial assessment of a possible screening test for decontaminated mask straps. This protocol could be implemented ahead of more complicated performance testing, allowing wide exploration of different mask types and decontamination protocols and progressing the important area of PPE reuse.

Author Contributions

Ian Pelse: conceptualization (supporting), data curation (lead), formal analysis (lead), investigation (lead), methodology (lead), resources (supporting), visualization (lead), writing – original draft (lead), writing – review and editing (equal). **Zach D. Seibers:** conceptualization (supporting), data curation (supporting), formal analysis (lead), investigation (lead), methodology (supporting), visualization (supporting), writing – original draft (supporting), writing – review and editing (equal). **John R. Reynolds:** conceptualization (equal), funding acquisition (equal), resources (equal), supervision (equal), writing – original draft (supporting), writing – review and editing (equal). **Meisha L. Shofner:** conceptualization (equal), data curation (supporting), formal analysis (supporting), funding acquisition (equal), resources (equal), supervision (equal), visualization (supporting), writing – original draft (supporting), writing – review and editing (equal).

Acknowledgments

This material is based on work supported by the National Science Foundation under Grant No. 2031545. The authors would like to thank the following people: Leanne West, for connecting us with other members of the community working on SARS-CoV-2 decontamination; Dr. M.G. Finn and Justin Lawrence, for connecting us with Walter Mann for ozone decontamination; Walter Mann of Zono Technologies for continuous use of the Zono Ozone cabinet; Dr. Brent Wagner of the Georgia Tech Research Institute for the use of his UV-C lamp and power meter; Dr. Tom Rosenmayer of Silpara Technologies for helpful discussions regarding elastomer degradation and mechanical testing; and Emily Ryan at Georgia Tech for her help throughout this project. This work was performed in part at the Materials Characterization Facility (MCF) at Georgia Tech. The MCF is jointly supported by the Institute for Materials (IMat) and the Institute for Electronics and Nanotechnology (IEN), which is a member of the National Nanotechnology Coordinated Infrastructure supported by the National Science Foundation (Grant

ECCS-2025462). FTIR was performed at the Organic Materials Characterization Laboratory (OMCL) at Georgia Tech.

Conflicts of Interest

The authors declare no conflicts of interest.

Data Availability Statement

The data that support the findings of this study are available from the corresponding author upon reasonable request.

References

1. R. J. Fischer, D. H. Morris, N. van Doremalen, et al., "Effectiveness of N95 Respirator Decontamination and Reuse against SARS-CoV-2 Virus," *Emerging Infectious Diseases* 26 (2020): 2253–2255.

2. G. Bagheri, B. Thiede, B. Hejazi, O. Schlenczek, and E. Bodenschatz, "An Upper Bound on One-To-One Exposure to Infectious Human Respiratory Particles," *Proceedings of the National Academy of Sciences of the United States of America* 118 (2021): e2110117118.

3. M. Jatta, C. Kiefer, H. Patolia, et al., "N95 Reprocessing by Low Temperature Sterilization With 59% Vaporized Hydrogen Peroxide During the 2020 COVID-19 Pandemic," *American Journal of Infection Control* 49 (2021): 8–14.

4. P. A. Kenney, B. K. Chan, K. E. Kortright, et al., "Hydrogen Peroxide Vapor Decontamination of N95 Respirators for Reuse," *Infection Control and Hospital Epidemiology* 43 (2022): 45–47.

5. J. J. Lowe, K. D. Paladino, J. D. Farke, et al., *N95 Filtering Facepiece Respirator Ultraviolet Germicidal Irradiation (UVGI) Process for Decontamination and Reuse*, Report from (Omaha, Nebraska: Nebraska Medicine, 2020).

6. W. G. Lindsley, S. B. Martin, R. E. Thewlis, et al., "Effects of Ultraviolet Germicidal Irradiation (UVGI) on N95 Respirator Filtration Performance and Structural Integrity," *Journal of Occupational and Environmental Hygiene* 12 (2015): 509–517.

7. L. Anderegg, C. Meisenhelder, C. O. Ngooi, et al., "A Scalable Method of Applying Heat and Humidity for Decontamination of N95 Respirators During the COVID-19 Crisis," *PLoS One* 15 (2020): e0234851.

8. L. Liao, W. Xiao, M. Zhao, et al., "Can N95 Respirators be Reused After Disinfection? How Many Times?," *ACS Nano* 14 (2020): 6348–6356.

9. E. L. Blanchard, J. D. Lawrence, J. A. Noble, et al., "Enveloped Virus Inactivation on Personal Protective Equipment by Exposure to Ozone," *medRxiv* (2020).

10. J. C. Rubio-Romero, M. d. C. Pardo-Ferreira, J. A. Torrecilla-García, and S. Calero-Castro, "Disposable Masks: Disinfection and Sterilization for Reuse, and Non-certified Manufacturing, in the Face of Shortages During the COVID-19 Pandemic," *Safety Science* 129 (2020): 104830.

11. J. Schwan, T. R. Alva, G. Nava, et al., "Efficient Facemask Decontamination via Forced Ozone Convection," *Scientific Reports* 11 (2021): 12263.

12. C. Cai, E. L. Floyd, and J. A. M. A. Netw, "Effects of Sterilization With Hydrogen Peroxide and Chlorine Dioxide Solution on the Filtration Efficiency of N95, KN95, and Surgical Face Masks," *Open* 3 (2020): e2012099–e2012099.

13. J. Driver, G. Lukasik, M. Bourgeois, P. Tam, and R. Harbison, "Virucidal Activity of Chlorine Dioxide gas for Reduction of Coronavirus on Surfaces and PPE," *Occupational Diseases and Environmental Medicine* 9 (2021): 13–19.

14. G. L. Robinson, S. Hitchcock, Z. Kpadeh-Rogers, et al., "Preventing Viral Contamination: Effects of Wipe and Spray-Based Decontamination of Gloves and Gowns," *Clinical Infectious Diseases* 69 (2019): S228–S230.

15. K. Lemmer, S. Howaldt, R. Heinrich, et al., "Test Methods for Estimating the Efficacy of the Fast-Acting Disinfectant Peracetic Acid on Surfaces of Personal Protective Equipment," *Journal of Applied Microbiology* 123 (2017): 1168–1183.

16. C. Jinadatha, S. Simmons, C. Dale, et al., "Disinfecting Personal Protective Equipment With Pulsed Xenon Ultraviolet as a Risk Mitigation Strategy for Health Care Workers," *American Journal of Infection Control* 43 (2015): 412–414.

17. *Historical Information about Device Emergency Use Authorizations*, https://www.fda.gov/medical-devices/emergency-use-authorizations-medical-devices/historical-information-about-device-emergency-use-authorizations#decontamination, accessed: May 25, 2023.

18. S. J. Volkoff, T. J. Carlson, K. Leik, et al., "Demonstrated SARS-CoV-2 Surface Disinfection Using Ozone," *Ozone: Science & Engineering* 43 (2021): 296–305.

19. E. P. Manning, M. D. Stephens, S. Dufresne, et al., "Disinfection of Pseudomonas Aeruginosa from N95 Respirators With Ozone: A Pilot Study," *BMJ Open Respiratory Research* 8 (2021): e000781.

20. W. J. Rogers, *Sterilisation of Biomaterials and Medical Devices*, eds. S. Lerouge and A. Simmons (Cambridge, UK: Woodhead Publishing, 2012), 151–211.

21. G. J. Lake and P. B. Lindley, "Role of Ozone in Dynamic Cut Growth of Rubber," *Journal of Applied Polymer Science* 9 (1965): 2031–2045.

22. W. F. Tuley, "Frosting of Vulcanized Rubber," *Industrial and Engineering Chemistry* 31 (1939): 714–716.

23. E. H. Andrews and M. Braden, "The Reaction of Ozone With Surfaces of Natural Rubber, and Its Dependence Upon Strain," *Journal of Polymer Science* 55 (1961): 787–798.

24. B. K. Heimbuch, W. H. Wallace, K. Kinney, et al., "A Pandemic Influenza Preparedness Study: Use of Energetic Methods to Decontaminate Filtering Facepiece Respirators Contaminated With H1N1 Aerosols and Droplets," *American Journal of Infection Control* 39 (2011): e1–e9.

25. M. B. Lore, B. K. Heimbuch, T. L. Brown, J. D. Wander, and S. H. Hinrichs, "Effectiveness of Three Decontamination Treatments against Influenza Virus Applied to Filtering Facepiece Respirators," *Annals of Occupational Hygiene* 56 (2011): 92–101.

26. D. F. Li, J. L. Cadnum, S. N. Redmond, L. D. Jones, and C. J. Donskey, "It's Not the Heat, it's the Humidity: Effectiveness of a Rice Cooker-Steamer for Decontamination of Cloth and Surgical Face Masks and N95 Respirators," *American Journal of Infection Control* 48 (2020): 854–855.

27. S. C. Daeschler, N. Manson, K. Joachim, et al., "Effect of Moist Heat Reprocessing of N95 Respirators on SARS-CoV-2 Inactivation and Respirator Function," *Canadian Medical Association Journal* 192 (2020): E1189–E1197.

28. C. Oh, E. Araud, J. V. Puthussery, et al., "Dry Heat as a Decontamination Method for N95 Respirator Reuse," *Environmental Science & Technology Letters* 7 (2020): 677–682.

29. M. Purschke, M. Elsamaloty, J. P. Wilde, et al., "Construction and Validation of UV-C Decontamination Cabinets for Filtering Facepiece Respirators," *Applied Optics* 59 (2020): 7585–7595.

30. D. Mills, D. A. Harnish, C. Lawrence, M. Sandoval-Powers, and B. K. Heimbuch, "Ultraviolet Germicidal Irradiation of Influenza-Contaminated N95 Filtering Facepiece Respirators," *American Journal of Infection Control* 46 (2018): e49–e55.

31. L. Mullins and N. R. Tobin, "Theoretical Model for the Elastic Behavior of Filler-Reinforced Vulcanized Rubbers," *Rubber Chemistry and Technology* 30 (1957): 555–571.

32. S. Cantournet, R. Desmorat, and J. Besson, "Mullins Effect and Cyclic Stress Softening of Filled Elastomers by Internal Sliding and Friction Thermodynamics Model," *International Journal of Solids and Structures* 46 (2009): 2255–2264.

33. F. H. A. Rodrigues, E. F. Santos, J. P. A. Feitosa, N. M. P. S. Ricardo, and R. C. M. d. Paula, "Ozonation of Unstretched Natural Rubber: Part I. Effect of Film Thickness," *Rubber Chemistry and Technology* 74 (2001): 57–68.

34. B. C. Smith, "The Infrared Spectra of Polymers IV: Rubbers," *Spectroscopy* 37 (2022): 8–12.

35. B. C. Smith, "Rolle der Vitamine im Alter – Evidenz und praktische Umsetzung," *Spectroscopy* 33 (2018): 20–23.

36. Y. Iwase, T. Shindo, H. Kondo, Y. Ohtake, and S. Kawahara, "Ozone Degradation of Vulcanized Isoprene Rubber as a Function of Humidity," *Polymer Degradation and Stability* 142 (2017): 209–216.

37. M. Alger, *Polymer Science Dictionary* (Dordrecht: Springer Science+Business Media, 2017).

38. S. D. Bruck, "Extension of the Flory-Rehner Theory of Swelling to an Anisotropic Polymer System," *Journal of Research of the National Bureau of Standards. Section A* 65A (1961): 485–487.

39. L. Valentine, "Interaction of Polyamides With Solvents. I. A Preliminary Survey of the Swelling of Crosslinked Nylon 66 in Various Types of Solvents," *Journal of Polymer Science* 23 (1957): 297–314.

Supporting Information

Additional supporting information can be found online in the Supporting Information section.